Astrophys Space Sci (2015) 355:245–251
DOI 10.1007/s10509-014-2180-8

ORIGINAL ARTICLE

Correlated observations and simulations on the buildup of radiation belt electron fluxes driven by substorm injections and chorus waves

Zhaoguo He · Hui Zhu · Siqing Liu · Qiugang Zong · Yongfu Wang · Ruilin Lin · Liqin Shi · Jiancun Gong

Received: 23 September 2014 / Accepted: 28 October 2014 / Published online: 5 December 2014

Abstract We report the multi-satellite (LANL, GOES-10 and Cluster) observation data of electron flux evolutions and chorus wave excitation in the radiation belt during the geomagnetic storm and substorm from 10 to 14 January, 2002. The seed (50–225 keV) electron flux increased 50 times in five hours during the storm main phase, and the relativistic (>0.6 MeV) electron flux increased about 60 times at night side during the recovery phase. In the meanwhile, the Cluster satellites detected intense chorus waves (the wave power up to $\sim 10^{-3}$ $nT^2\,Hz^{-1}$) at MLT ≈ 3 when passing through the outer radiation belt. Using a Gaussian fit to the observed chorus spectra, we calculate the drift-averaged diffusion coefficients and then solve a 2-D Fokker-Planck diffusion equation. We simulate the energetic electron flux evolutions driven by chorus waves in two cases: with and without seed electron injections. We show that the energetic electron flux increases 79 times in three days with injection, comparable to the observation. However, the flux increases only 3 times in three days without injection, far below the observation. The current results suggest that the injected seed electrons and chorus waves play important roles in the buildup of the radiation belt electrons.

Z. He · S. Liu (✉) · R. Lin · L. Shi · J. Gong
Center for Space Science and Applied Research,
Chinese Academy of Sciences, Beijing, 100190, China
e-mail: liusq@nssc.ac.cn

H. Zhu
CAS Key Laboratory of Geospace Environment,
Department of Geophysics and Planetary Sciences,
University of Science and Technology of China, Hefei, Anhui,
230026, China

Q. Zong · Y. Wang
Institute of Space Physics and Applied Technology,
Peking University, Beijing, 100871, China

Keywords Radiation belt · Substorm · Seed electron injection · Chorus waves · Acceleration · Energetic electron

1 Introduction

The radiation belt energetic (>0.1 MeV) electrons are usually distributed in two distinct regions: slowly evolving inner belt ($1.2 < L < 2$) and highly dynamic outer belt ($3 < L < 7$). The third radiation belt can arise under extreme conditions (Blake et al. 1992; Baker et al. 2013). During the geomagnetically active periods, these energetic electron fluxes in the outer belt can vary by several orders of magnitude over timescales ranging from hours to days (Baker et al. 1986; Li et al. 1997). Such dramatic variation is determined by the competition and cooperation of various loss, acceleration and transport processes (Reeves et al. 2003). Understanding the physical processes of the energetic electron flux variation have both scientific and practical significance, considering its serious impacts on the space environment (e.g., harming the spacecrafts in the inner magnetosphere) (Baker 2002).

The cyclotron resonance with whistler-mode chorus waves has been considered to be the most important acceleration mechanism for the radiation belt electrons (Summers et al. 1998; Horne and Thorne 1998; Thorne et al. 2013; Gao et al. 2014). The chorus waves are generally distributed outside the plasmasphere over magnetic local time (MLT) from 2300 MLT through 0600 MLT to 1400 MLT with typical frequencies 0.05–0.80 f_{ce} (f_{ce} is the equatorial electron gyrofrequency) (Thorne et al. 2007). Depending on plasma density and wave spectrum, chorus can resonate with electrons in a wide energy range from ~keV to a few MeV (Summers et al. 1998; Horne and Thorne 1998; Ni et al. 2008; Su et al. 2009b, 2010a; Thorne et al. 2010). The quasi-linear kinetic

model has been widely used to quantitatively describe the chorus acceleration process (e.g., Albert 2003, 2004, 2005; Albert et al. 2009; Summers et al. 2002; Summers 2005; Horne et al. 2005; Li et al. 2007; Shprits et al. 2006, 2009; Xiao et al. 2009, 2014; Su et al. 2009a, 2009c, 2014a; Yan et al. 2013). These numerical studies have shown that the chorus waves can accelerate ∼100 keV seed electrons to ∼MeV radiation belt electrons on a timescale of days.

The short-period substorm process is able to inject the tens to hundreds keV electrons from the magnetic tail into the radiation belt region (McIlwain 1974; Friedel et al. 1996; Reeves et al. 1996; Liu et al. 2003). The injected anisotropic lower energy electrons (<100 keV) provide the free energy to generate chorus waves (Tsurutani and Smith 1977; Meredith et al. 2001; Lauben et al. 2002; Li et al. 2009; Su et al. 2014b). Subsequently, the injected higher energy (100–200 keV) electrons can be accelerated to the relativistic electrons by chorus waves.

The quasi-linear simulations on the chorus acceleration have been implemented by several research groups. Recent study (Zhang et al. 2014) provided a parametric study on the effect of low energy electron injection on storm-time evolution of radiation belt energetic electrons. However, simultaneous observation and corresponding modeling of radiation belt electron dynamics driven by substorm injection and chorus waves have seldom been reported. In this paper, we study a specific event of radiation belt flux buildup during a geomagnetic storm accompanied with prolonged substorm activities. Based on both observations and simulations, we attempt to identify the respective contributions of substorm injection and chorus wave acceleration for the radiation belt electron flux enhancement.

2 Observations

We select the radiation belt storm event during 10–14 January, 2002. An overview of this event is shown in Fig. 1. Figure 1a and 1b show the *Dst* and *AE* indices provided by the CDAweb-OMNI database (http://cdaweb.gsfc.nasa.gov/cdaweb/istp_public/). A multi-steps storm occurred on 10 January, with the minimum *Dst* value of −72 nT at 06:30 UT on 11 January. Meanwhile, the prolonged substorm activity occurred, with the maximum *AE* value of 1600 nT during the main phase of the storm. Figure 1c plots the electron (50–225 keV) flux data observed by the SPA (Synchronous Orbit Particle Analyzer) (Belian et al. 1992) of the LANL (Los Alamos National Laboratory) satellite at the geosynchronous orbit. Throughout the storm, the flux enhancements were closely related to the increases in *AE* index, indicating the injections of low energy electrons during the substorms. For example, the flux increased by about 50 times in five hours from 12:00 UT to 17:00 UT on 10 January, corresponding to the peak time of *AE* index. Figure 1d and 1e exhibit the power spectral densities of magnetic field observed by STAFF instruments (Cornilleau-Wehrlin et al. 2003) onboard the Cluster C3 and C4 satellites. The Cluster satellites have highly elliptical polar orbits, with $4R_E$ perigee and $19.6R_E$ apogee (R_E is the Earth radius). The orbital period is about 57 hours, but the travel time in the outer radiation belt is only about 2 hours for each orbit. During the periods from 19:20 UT to 20:40 UT and 21:00 UT to 22:20 UT on 10 January, strong lower band ($< 0.5 f_{ce}$) chorus waves were observed in the nightside (MLT ≈ 3) low-latitude region, with the intensity up to $\sim 10^{-3}$ nT^2/Hz and the frequency range from 100 Hz to 4000 Hz. The chorus waves may be generated by those injected low energy electrons (Tsurutani and Smith 1977; Lauben et al. 2002; Miyoshi et al. 2003). Figure 1f presents the simultaneous observation of energetic electron flux by EPS (Energetic Particle Sensor) (Onsager et al. 1996) of GOES-10 (Geostationary Operational Environmental Satellite). The flux of >0.6 MeV electron decreased during main phase and increased rapidly during the recovery phase. The daily periodic fluctuations are probably caused by the day-night asymmetric structure of the magnetosphere (Reeves et al. 1998). The flux dropout in the main phase may be explained by the adiabatic transport, outward radial diffusion and magnetopause shadowing (Kim and Chan 1997; Shprits and Thorne 2004; Su et al. 2011a). Here we focus on the flux buildup during the recovery phase. In the nightside region (gray shadows), the energetic electron flux increased about 60 times within three days. The seed electron injection and the following chorus-driven acceleration can be expected to account for the energetic electron flux enhancement.

3 Simulations

Here we use the quasi-linear model STEERB (Xiao et al. 2009, 2010; Su et al. 2009a, 2010c, 2010b, 2011a, 2011b) to simulate the energetic electron flux buildup at $L = 6.6$. This model can quantify the electron phase space density (PSD) f evolution by solving the two-dimensional Fokker-Planck equation (Kozyra et al. 1994):

$$\frac{\partial f}{\partial t} = \frac{1}{Gp}\frac{\partial}{\partial \alpha_e}\left[G\left(\langle D_{\alpha\alpha}\rangle \frac{1}{p}\frac{\partial f}{\partial \alpha} + \langle D_{\alpha p}\rangle \frac{\partial f}{\partial p}\right)\right] + \frac{1}{G}\frac{\partial}{\partial p}\left[G\left(\langle D_{p\alpha}\rangle \frac{1}{p}\frac{\partial f}{\partial \alpha_e} + \langle D_{pp}\rangle \frac{\partial f}{\partial p}\right)\right] - \frac{f}{\tau_L}, \quad (1)$$

with

$$G = p^2 T(\alpha_e) \sin\alpha_e \cos\alpha_e, \quad (2)$$

$$T = 1.3 - 0.56 \sin\alpha_e, \quad (3)$$

where α_e represent equatorial pitch angle; p is the momentum of electrons; $\langle D_{\alpha\alpha}\rangle$, $\langle D_{pp}\rangle$ and $\langle D_{\alpha p}\rangle = \langle D_{p\alpha}\rangle$ are the

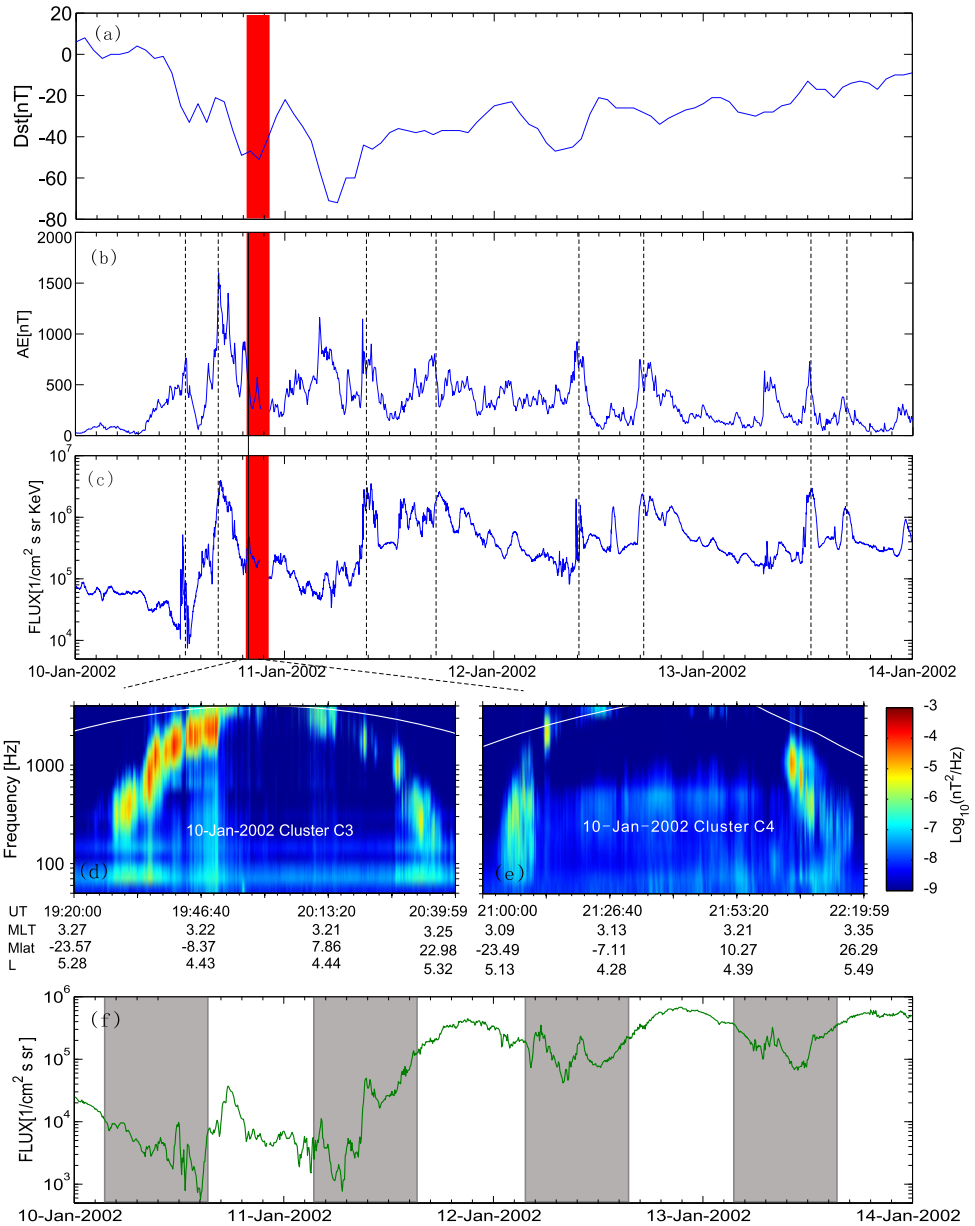

Fig. 1 (**a**) *Dst* index; (**b**) *AE* index; (c) Flux of 50–225 keV electron observed by LANL; (**d**)–(**e**) Chorus waves observed by Cluster C3 and C4, the white line denote 0.5 f_{ce}; (f) Evolution of energetic electron (>0.6 MeV) flux observed by GOES-10. The shadows in *red* in panels a, b and c are the periods when chorus waves are detected. The shadows in *gray* in panel f denote the periods when the satellite flew through nightside of the earth

drift-averaged pitch-angle, momentum and cross diffusion coefficients of chorus waves, respectively. The term $-f/\tau_L$ indicates the electron precipitation in the loss cone, and τ_L is the electron life time with a quarter of bounce period.

The simulation domain is taken as $[0°, 90°] \times [0.05, 5.0]$ MeV in the space (α_e, E_k). The initial PSD f_w is assumed to obey the Kappa distribution (Vasyliunas 1968; Viñas et al. 2005; Xiao et al. 2008a, 2008b)

$$f_w = C\left(\frac{p\sin\alpha_e}{\theta_\kappa}\right)^{2l}\left[1+\frac{p^2}{\kappa\theta_\kappa^2}\right]^{-(\kappa+l+1)}, \tag{4}$$

$$C = \frac{N\Gamma(\kappa+l+1)}{\pi^{3/2}\theta_\kappa^3\kappa^{(l+3/2)}\Gamma(l+1)\Gamma(\kappa-1/2)}, \tag{5}$$

where l is the loss cone index, θ_κ^2 is the effective thermal parameter, κ is the spectral index, N is the number density, and Γ is gamma function. These parameters are set to be l = 0.5, $\theta_\kappa^2 = 0.023$, $\kappa = 3$ and $N = 0.1$ cm^{-3}, roughly determined by the observed differential fluxes of LANL and GOES-10 at three different energy channels (as shown in Fig. 2). The equivalent extrapolation is applied at the two pitch-angle boundaries. The PSD is fixed at the upper momentum boundary, but time-dependent at the lower momentum boundary due to the substorm injection of seed electrons. The PSD of low energy (50–225 keV) is assumed to increase 50 times in 5 hours, namely

$$f_e = f_w(1+49t/5), \quad t \le 5h \tag{6}$$

where t is in units of hour.

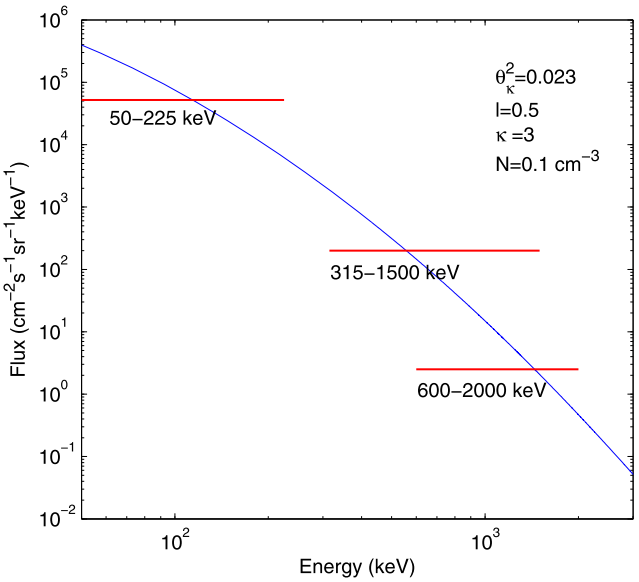

Fig. 2 The *red horizontal lines* show the initial differential fluxes of the three energy channels from LANL and GOES-10 observations. The fluxes are taken as the average values from 00:00 UT to 12:00 UT on 10 January. The *blue curve* denotes the Kappa distribution with $\theta_\kappa^2 = 0.023$, $l = 0.5$, $\kappa = 3$ and $N = 0.1$ cm^{-3}

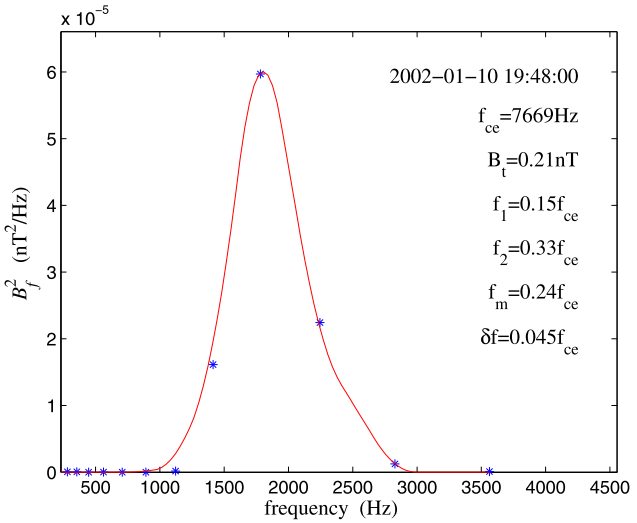

Fig. 3 The modeled Gaussian fit (*solid*) to the observed wavespectra (*dot*)

A typical Gaussian distribution is used to model the wave spectral density as a function of frequency. Figure 3 shows a least squares Gaussian fit (solid) to the observed chorus spectral intensity (dotted) by Cluster C3 at 19:48 UT on 10 January, together with the corresponding best fitting values of parameters: the wave amplitude $B_t = 0.21$ nT, the center frequency $f_m = 0.24 f_{ce}$, the half width $\delta_f = 0.045 f_{ce}$, the lower band $f_1 = 0.15 f_{ce}$, and the upper band $f_2 = 0.33 f_{ce}$. The distribution of normal angle tangent ($X = \tan\theta$) is assumed to follow the Gaussian distribution with peak $X_m = 0$, bandwidth $X_w = \tan 30°$, lower band $X_1 = 0$ and upper band $X_2 = 1$. The important parameter ω_{pe}/Ω_e is adopted to be 3.2. Figure 4 displays the drift-averaged diffusion coefficients for the modeled chorus waves. The distribution characteristics are similar to those in the early works (Li et al. 2007; Shprits et al. 2009; Su et al., Xiao et al. 2009a, 2009). These diffusion coefficients peak at the large equatorial pitch angles, indicating the strong acceleration effect on the trapped electrons.

We simulate the evolutions of energetic electron PSD driven by chorus waves under two conditions: with and without seed electron injections. Figure 5 shows the initial and final PSD profiles as a function of equatorial pitch angle at $E_k = 0.8$ MeV, 1 MeV, 1.5 MeV and 2 MeV for the two simulation cases. The chorus waves lead to obvious increase of energetic electron PSD after three days, especially for large pitch angle of 0.8 MeV and 1 MeV electrons. This is reasonable since the PSD evolution is essentially controlled by the diffusion terms, and the diffusion coefficients in the region of $\alpha_e > 60°$ and $E_k < 1$ MeV are generally one order larger than those coefficients outside this region. Moreover, the PSD of 0.8 MeV, 1 MeV and 1.5 MeV electron with injections are found to be a factor of 20, 10 and 2 higher than those without injections for $\alpha_e > 60°$. There are no significant changes between with and without injections for 2 MeV electrons.

A detailed comparison between the simulation and observation of the >0.6 MeV electron fluxes $j = p^2 f$ is shown in Fig. 6. Note that the electron fluxes are normalized by the initial values. Obviously, without substorm injection, the simulated flux is only approximately one thirtieth of the observed flux at $t = 3$ days. Including the injection, the simulated flux is slightly less than the observation at $t = 0.5$ day, but consistent with the observation at $t = 3$ days. To test the sensitivity of simulation on the wave amplitude, the wave amplitude is increased by a factor of $\sqrt{2}$ (i.e., the diffusion coefficients are increased by 2 times). The increased chorus waves, together with the substorm injection, can well explain the flux enhancement in the first day, but significantly overestimate the flux at $t = 3$ days. These results indicate that both the substorm injection and proper chorus waves are important for the radiation belt dynamics.

4 Summary

We study the buildup of radiation belt electron fluxes during a multi-step storm from 10 to 14 January, 2002. The electron flux variations were observed by LANL and GOES-10, and the chorus wave activities were simultaneously detected by the Cluster satellites. Seed electron (50–225 keV)

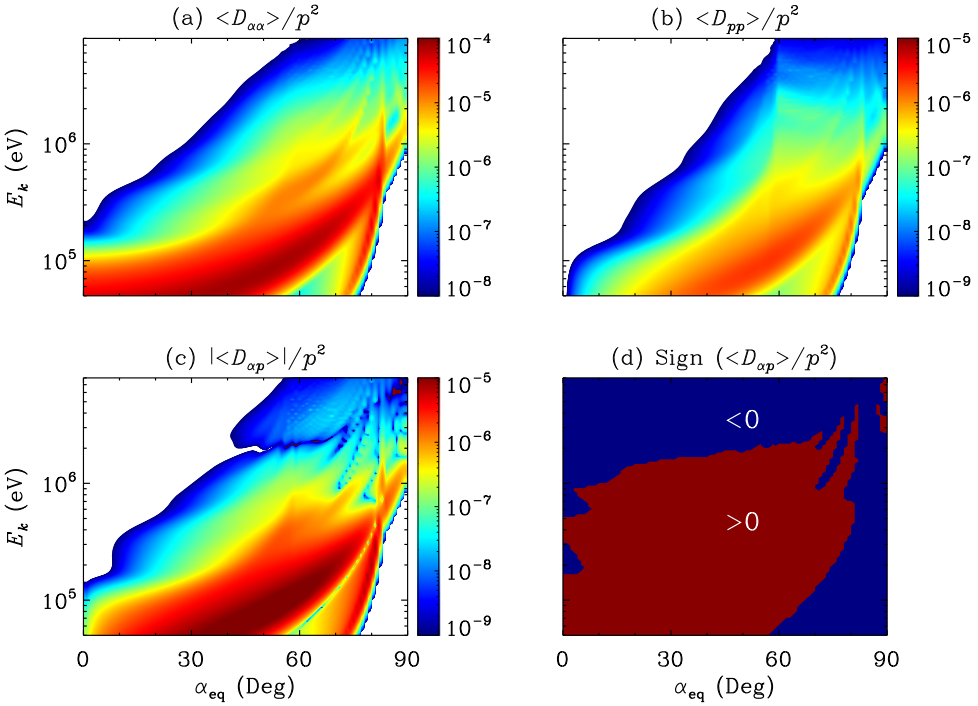

Fig. 4 Drift-averaged diffusion coefficients of (**a**) pitch angle, (**b**) momentum, (**c**) cross in units of s^{-1}, as the function of energy and pitch angle, and (**d**) the sign of the cross diffusion coefficient

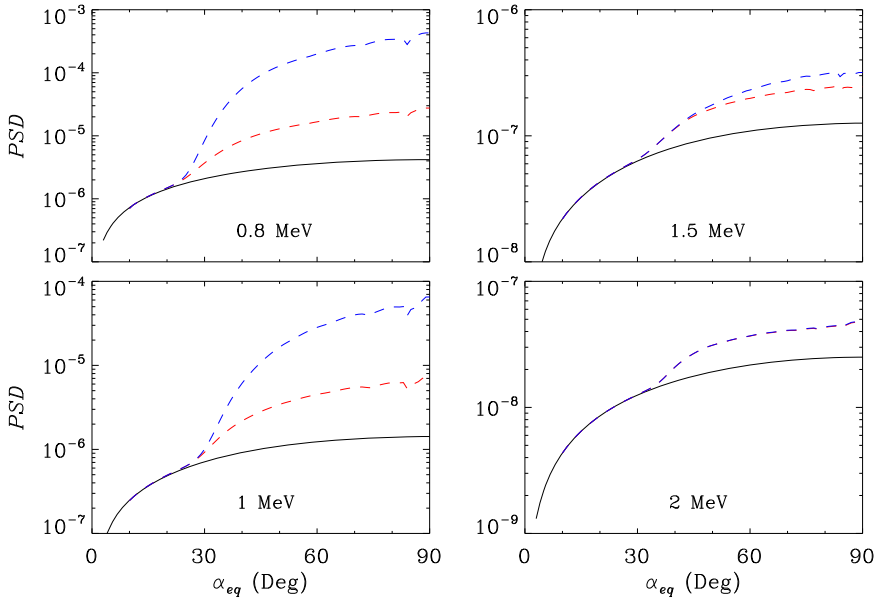

Fig. 5 The PSD (in arbitrary units) evolutions of electrons for $E_k = 0.8$, 1.5, 1 and 2 MeV. The *solid* and *dash lines* denote the PSD at initial time and after 3 days. The *red* and *blue lines* represent evolutions without and with injections, respectively

flux at geostationary orbit observed by LANL increased 50 times during the storm, and the chorus waves were excited in the outer radiation belt with the amplitude $B_t = 0.21$ nT and frequency ranging from $0.1\,f_{ce}$ to $0.5\,f_{ce}$. The relativistic electron (>0.6 MeV) flux increased about 60 times in three days. The data-driven simulations are performed by the STEERB code to identify the respective contributions of substorm injection and chorus acceleration for the radiation belt electron flux enhancement. With substorm injection, chorus waves can produce remarkable flux enhancements at larger pitch angle range (by about 100 times for 0.8 MeV, 40 times for 1 MeV, 3 times for 1.5 MeV and 1.5 times for 2 MeV), generally consistent with the observation. Without substorm injection, the chorus waves can only slightly increase the electron flux. These simulation results clearly demonstrate the synergistic effect of substorm injections and chorus waves on radiation belt evolution.

Acknowledgements This work was supported by 973 program 2012CB25600 and 2011CB811406. We thank the CDAWeb and Cluster science teams for the data used in this study.

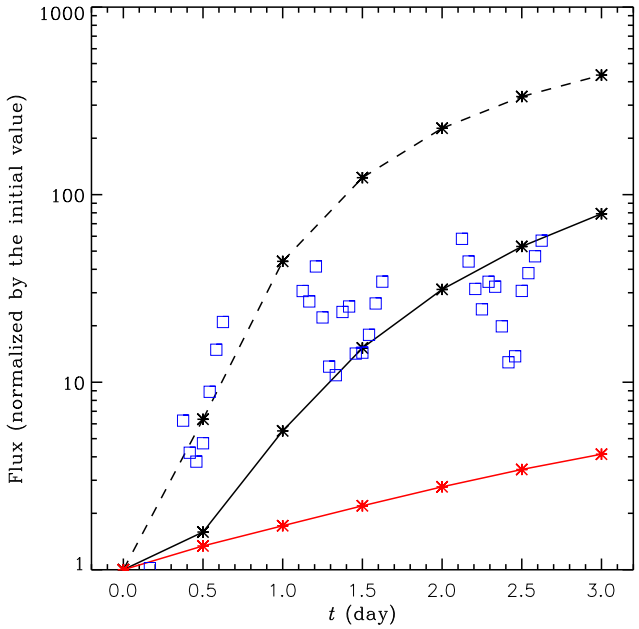

Fig. 6 Detailed comparisons of simulated and observation energetic electron evolutions normalized by their initial values. The *black* and *red lines* denote the fluxes with and without injections. The *black dot line* denotes the flux evolution with doubled diffusion coefficients (a factor of $\sqrt{2}$ for wave amplitude). The *star symbols* represent the simulation results and the *square symbols* are the observation data from GOES-10 in the nightside region

References

Albert, J.M.: J. Geophys. Res. **108**(A8), 1249 (2003). doi:10.1029/2002JA009792

Albert, J.M.: Space Weather **2**, 9 (2004). doi:10.1029/2004SW000069

Albert, J.M.: J. Geophys. Res. **110**(A9), 03218 (2005). doi:10.1029/2004JA010844

Albert, J.M., Meredith, N.P., Horne, R.B.: J. Geophys. Res. **114**, 09214 (2009). doi:10.1029/2009JA014336

Baker, D.N.: Science **297**(5586), 1486 (2002)

Baker, D.N., Blake, J.B., Klebesadel, R.W., Higbie, P.R.: J. Geophys. Res. **91**, 4265 (1986)

Baker, D.N., Kanekal, S.G., Hoxie, V.C., Henderson, M.G., Li, X., Spence, H.E., Elkington, S.R., Friedel, R.H.W., Goldstein, J., Hudson, M.K., et al.: Science **340**(6129), 186 (2013)

Belian, R.D., Gisler, G.R., Cayton, T., Christensen, R.: J. Geophys. Res. **97**, 16897 (1992)

Blake, J.B., Kolasinski, W.A., Fillius, R.W., Mullen, E.G.: Geophys. Res. Lett. **19**, 821 (1992). doi:10.1029/92GL00624

Cornilleau-Wehrlin, N., Chanteur, G., Perraut, S., Rezeau, L., Robert, P., Roux, A., de Villedary, C., Canu, P., Maksimovic, M., de Conchy, Y., Hubert, D., Lacombe, C., Lefeuvre, F., Parrot, M., Pincon, J.L., Decreau, P.M.E., Harvey, C.C., Louarn, P., Santolik, O., Alleyne, H.S.C., Roth, M., Chust, T., Contel, O.L., team, S.: Ann. Geophys. **21**, 437 (2003). doi:10.5194/angeo-21-437-2003

Friedel, R., Korth, A., Kremser, G.: J. Geophys. Res. **101**(A6), 13137 (1996)

Gao, Z., Zhu, H., Zhang, L., Zhou, Q., Yang, C., Xiao, F.: Astrophys. Space Sci. **351**(2), 427 (2014). doi:10.1007/s10509-014-1859-1

Horne, R.B., Thorne, R.M.: Geophys. Res. Lett. **25**, 3011 (1998)

Horne, R.B., Thorne, R.M., Glauert, S.A., Albert, J.M., Meredith, N.P., Anderson, R.R.: J. Geophys. Res. **110**, 03225 (2005). doi:10.1029/2004JA010811

Kim, H.-J., Chan, A.A.: J. Geophys. Res. **102**, 22107 (1997). doi:10.1029/97JA01814

Kozyra, J.U., Rasmussen, C.E., Miller, R.H., Lyons, L.R.: J. Geophys. Res. **99**, 4069 (1994)

Lauben, D.S., Inan, U.S., Bell, T.F., Gurnett, D.A.: J. Geophys. Res. **107**, 1429 (2002). doi:10.1029/2000JA003019

Li, X., Baker, D.N., Temerin, M., Cayton, T.E., Reeves, G.D., Christensen, R.A., Blake, J.B., Looper, M.D., Nakamura, R., Kanekal, S.G.: J. Geophys. Res. **102**, 14123 (1997)

Li, W., Shprits, Y.Y., Thorne, R.M.: J. Geophys. Res. **112**, 10220 (2007). doi:10.1029/2007JA012368

Li, W., Thorne, R.M., Angelopoulos, V., Bonnell, J.W., McFadden, J.P., Carlson, C.W., LeContel, O., Roux, A., Glassmeier, K.H., Auster, H.U.: J. Geophys. Res. **114**, 00 (2009). doi:10.1029/2008JA013554

Liu, S., Chen, M.W., Korth, L.R.L.H., Albert, J.M., Roeder, J.L., Anderson, P.C., Thomsen, M.F.: J. Geophys. Res. **108**, 1372 (2003). doi:10.1029/2003JA010004

McIlwain, C.E.: In: McCormac, B.M. (ed.) Magnetospheric Physics, p. 143 (1974)

Meredith, N.P., Horne, R.B., Anderson, R.R.: J. Geophys. Res. **106**, 13165 (2001)

Miyoshi, Y., Morioka, A., Obara, T., Misawa, H., Nagai, T., Kasahara, Y.: J. Geophys. Res. **108**(A1), 1004 (2003). doi:10.1029/2001JA007542

Ni, B., Thorne, R.M., Shprits, Y.Y., Bortnik, J.: Geophys. Res. Lett. **35**, 11106 (2008). doi:10.1029/2008GL034032

Onsager, T., Grubb, R., Kunches, J., Matheson, L., Speich, D., Zwickl, R.W., Sauer, H.: Proc. SPIE **2812**, 281 (1996). doi:10.1117/12.254075

Reeves, G.D., Henderson, M.G., McLachlan, P.S., Belian, R.D., Friedel, R.H.W., Korth, A.: In: Rolfe, E.J., Kaldeich, B. (eds.) International Conference on Substorms. ESA Special Publication, vol. 389, p. 579 (1996)

Reeves, G.D., Friedel, R.H.W., Belian, R.D., Meiet, M.M., Henderson, M.G., Onsager, T., Singer, H.J., Baker, D.N., Li, X., Blake, J.B.: J. Geophys. Res. **103**, 17559 (1998)

Reeves, G.D., McAdams, K.L., Friedel, R.H.W., O'Brien, T.P.: Geophys. Res. Lett. **30**(10), 1529 (2003). doi:10.1029/2002GL016513

Shprits, Y.Y., Thorne, R.M.: Geophys. Res. Lett. **31**, 08805 (2004). doi:10.1029/2004GL019591

Shprits, Y.Y., Thorne, R.M., Horne, R.B., Glauert, S.A., Cartwright, M., Russell, C.T., Baker, D.N., Kanekal, S.G.: Geophys. Res. Lett. **33**, 05104 (2006). doi:10.1029/2005GL024256

Shprits, Y.Y., Subbotin, D., Ni, B.: J. Geophys. Res. **114**, 11209 (2009). doi:10.1029/2008JA013784

Su, Z., Zheng, H., Wang, S.: J. Geophys. Res. **114**, 07201 (2009a). doi:10.1029/2008JA014013

Su, Z., Zheng, H., Wang, S.: J. Geophys. Res. **114**, 08202 (2009b). doi:10.1029/2009JA014269

Su, Z., Zheng, H., Chen, L., Wang, S.: J. Atmos. Sol.-Terr. Phys. **73**, 95 (2009c). doi:10.1016/j.jastp.2009.08.002

Su, Z., Zheng, H., Wang, S.: J. Geophys. Res. **115**, 05219 (2010a). doi:10.1029/2009JA014759

Su, Z., Xiao, F., Zheng, H., Wang, S.: J. Geophys. Res. **115**, 10249 (2010b). doi:10.1029/2010JA015903

Su, Z., Xiao, F., Zheng, H., Wang, S.: J. Geophys. Res. **115**, 09208 (2010c). doi:10.1029/2009JA015210

Su, Z., Xiao, F., Zheng, H., Wang, S.: Geophys. Res. Lett. **38**, 06106 (2011a). doi:10.1029/2011GL046873

Su, Z., Xiao, F., Zheng, H., Wang, S.: J. Geophys. Res. **116**, 04205 (2011b). doi:10.1029/2010JA016228

Su, Z., Xiao, F., Zheng, H., He, Z., Zhu, H., Zhang, M., Shen, C., Wang, Y., Wang, S., Kletzing, C.A., Kurth, W.S., Hospodarsky, G.B., Spence, H.E., Reeves, G.D., Funsten, H.O., Blake, J.B., Baker, D.N.: Geophys. Res. Lett. **41**, 229 (2014a). doi:10.1002/2013GL058912

Su, Z., Zhu, H., Xiao, F., Zheng, H., Wang, Y., He, Z., Shen, C., Shen, C., Wang, C.B., Liu, R., Zhang, M., Wang, S., Kletzing, C.A., Kurth, W.S., Hospodarsky, G.B., Spence, H.E., Reeves, G.D., Funsten, H.O., Blake, J.B., Baker, D.N., Wygant, J.R.: J. Geophys. Res. **119**(6), 4266 (2014b). doi:10.1002/2014JA019919

Summers, D.: J. Geophys. Res. **110**, 08213 (2005). doi:10.1029/2005JA011159

Summers, D., Thorne, R.M., Xiao, F.: J. Geophys. Res. **103**, 20487 (1998)

Summers, D., Ma, C., Meredith, N.P., Horne, R.B., Thorne, R.M., Heynderickx, D., Anderson, R.R.: Geophys. Res. Lett. **29**(24), 2174 (2002). doi:10.1029/2002GL016039

Thorne, R.M., Shprits, Y.Y., Meredith, N.P., Horne, R.B., Li, W., Lyons, L.R.: J. Geophys. Res. **112**, 06203 (2007). doi:10.1029/2006JA012176

Thorne, R.M., Ni, B., Tao, X., Horne, R.B., Meredith, N.P.: Nature **467**, 943 (2010). doi:10.1038/nature09467

Thorne, R.M., Li, W., Ni, B., Ma, Q., Bortnik, J., Chen, L., Baker, D.N., Spence, H.E., Reeves, G.D., Henderson, M.G., Kletzing, C.A., Kurth, W.S., Hospodarsky, G.B., Blake, J.B., Fennell, J.F., Claudepierre, S.G., Kanekal, S.G.: Nature **504**, 411 (2013). doi:10.1038/nature12889

Tsurutani, B.T., Smith, E.J.: J. Geophys. Res. **82**, 5112 (1977)

Vasyliunas, V.M.: J. Geophys. Res. **73**, 2839 (1968)

Viñas, A.F., Mace, R.L., Benson, R.F.: J. Geophys. Res. **110**, 06202 (2005). doi:10.1029/2004JA010967

Xiao, F., Chen, L., Li, J.: Plasma Phys. Control. Fusion **50**, 105002 (2008a). doi:10.1088/0741-3335/50/10/105002

Xiao, F., Shen, C., Wang, Y., Zheng, H., Wang, S.: J. Geophys. Res. **113**, 05203 (2008b). doi:10.1029/2007JA012903

Xiao, F., Su, Z., Zheng, H., Wang, S.: J. Geophys. Res. **114**, 03201 (2009). doi:10.1029/2008JA013580

Xiao, F., Su, Z., Zheng, H., Wang, S.: J. Geophys. Res. **115**, 05216 (2010). doi:10.1029/2009JA014541

Xiao, F., Yang, C., He, Z., Su, Z., Zhou, Q., He, Y., Kletzing, C.A., Kurth, W.S., Hospodarsky, G.B., Spence, H.E., Reeves, G.D., Funsten, H.O., Blake, J.B., Baker, D.N., Wygant, J.R.: J. Geophys. Res. **119**, 3325 (2014). doi:10.1002/2014JA019822

Yan, Q., Shi, L., Liu, S.: Sci. China, Technol. Sci. **56**(2), 492 (2013). doi:10.1007/s11431-012-5078-0

Zhang, Y., Zhu, H., Zhang, L., He, Y., Gao, Z., Zhou, Q., Yang, C., Xiao, F.: Astrophys. Space Sci. **352**(2), 613 (2014). doi:10.1007/s10509-014-1984-x